Frontiers of Information Technology & Electronic Engineering
www.jzus.zju.edu.cn; engineering.cae.cn; www.springerlink.com
ISSN 2095-9184 (print); ISSN 2095-9230 (online)
E-mail: jzus@zju.edu.cn

Supplementary Materials for

Fanghao HUANG, Xiao YANG, Xuanlin CHEN, Deqing MEI, Zheng CHEN, 2025. A digital simulation platform with human-interactive immersive design for navigation, motion, and teleoperated manipulation of work-class remotely operated vehicle. *Front Inform Technol Electron Eng*, 26(8):1394-1410.
https://doi.org/10.1631/FITEE.2400486

1 Design of the teleoperated manipulation unit

1.1 System modeling

In the teleoperation system, the master manipulator is selected as Omni, and the slave manipulator is the manipulator equipped on the ROV, which has six joints and one gripper. For the master manipulator, the position of the end effector for the master manipulator can be directly obtained from the Omni driver.

For the slave manipulator, consider the following dynamics in Cartesian space:

$$M_s(q_s)\ddot{X}_s + C_s(q_s,\dot{q}_s)\dot{X}_s + G_s(q_s) + D_s = T_s + F_e, \tag{S1}$$

where X_s, $\dot{X}_s$, $\ddot{X}_s$ represent the position, velocity, and acceleration of the slave manipulator, respectively; M_s, C_s, and G_s are the mass inertia matrix, Coriolis/centrifugal matrix, and gravity matrix, respectively. D_s represents disturbance and modeling errors. T_s stands for the input signals of the manipulators, and F_e is the environmental force.

Property 1 $\dot{M}_s - 2C_s$ is the skew-symmetric matrix.

Property 2 Part of Eq. (S1) can be written in the form of a radial basis function neural network (RBFNN) as follows:

$$M_s(q_s)\ddot{X}_{sd} + C_s(q_s,\dot{q}_s)\dot{X}_{sd} + G_s(q_s) = W_s^T H_s(q_s,\dot{q}_s,\dot{X}_{sd},\ddot{X}_{sd}), \tag{S2}$$

where X_{sd} represents the desired trajectory of the slave manipulator. $W_s^T = diag\{W_1^T,\ldots,W_r^T,\ldots,W_n^T\}$, $r = 1,\ldots,n$ is the controlled degree of freedom of the slave manipulators; W_r is the vector of ideal weights of the RBFNN; $H_s(z) = \left[H_1^T(z_1),\ldots,H_r^T(z_r),\ldots,H_n^T(z_n)\right]^T$, and z is the input of RBFNN, $H_r(z_r)$ is the vector of radial basis functions.

Assumption 1 The disturbance and modeling errors are bounded by $\|D_s\| \le \bar{d}_s$.

1.2 Teleoperation control framework

To enhance the telepresence experience for the human operator during the operation mode, visual and force feedbacks are commonly adopted. However, since unavoidable time delays exist in the teleoperation process, bidirectional data transmission (velocity and force signals) between the master and the slave sides may deteriorate the stability of teleoperation (Hokayem and Spong, 2006). As a result, a modified wave-variable architecture is utilized to ensure the stability of the teleoperation system. We define the position and velocity of the master as X_m and $\dot{X}_m$, respectively, and F_e and F_m are the environmental force in the slave side and its force feedback to the master side, respectively.

As shown in Fig.S1, the transmitted signals are replaced by u_m and v_s, which can be described as

follows:

$$u_m(t) = \frac{b\dot{X}_m(t) + F_e(t - T_{sm})}{\lambda} \bigotimes L^{-1}(\frac{1}{\tau s + 1}), \tag{S3}$$

$$v_s(t) = \frac{F_e(t)}{\lambda}. \tag{S4}$$

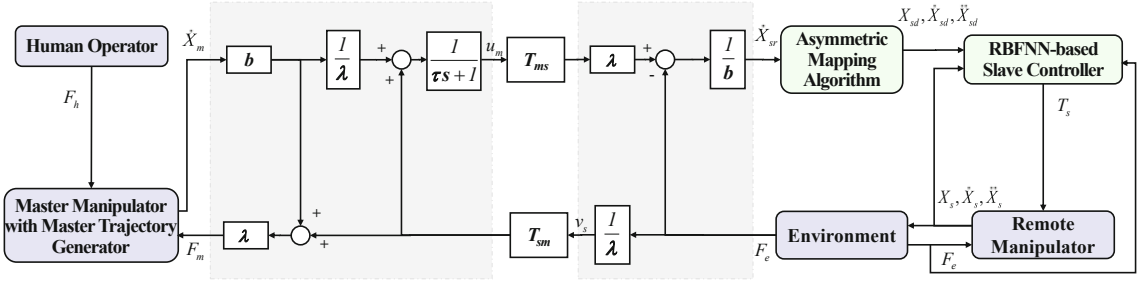

Fig. S1 Teleoperation control framework

Therefore, the signals received in the slave side and master side can be obtained as:

$$\dot{X}_{sr}(t) = \frac{\lambda u_m(t - T_{ms}) - F_e(t)}{b}, \tag{S5}$$

$$F_m(t) = \lambda \left(v_s(t - T_{sm}) + b\dot{X}_m(t) \right). \tag{S6}$$

Substituting Eqs. (S3) and (S4) into Eqs. (S5) and (S6), one can obtain the following:

$$\begin{aligned} \dot{X}_{sr}(t) = &\left(\dot{X}_m(t - T_{ms}) + \frac{1}{b} F_e(t - T_{ms} - T_{sm}) \right) \\ &\bigotimes L^{-1}(\frac{1}{\tau s + 1}) - \frac{1}{b} F_e(t), \end{aligned} \tag{S7}$$

$$F_m(t) = F_e(t - T_{sm}) + b\lambda \dot{X}_m(t). \tag{S8}$$

Since the wave variables are introduced as in Eqs. (S3) and (S4), the following hybrid matrix of the wave-variable-based teleoperation system can be obtained.

$$M(s) = \begin{bmatrix} b\lambda & e^{-sT_{sm}} \\ -\frac{e^{-sT_{ms}}}{\tau s + 1} & \frac{1}{b} - \frac{e^{-s(T_{ms} + T_{sm})}}{b(\tau s + 1)} \end{bmatrix}. \tag{S9}$$

According to the scattering operator theory (Anderson and Spong, 1989), we define the scattering matrix as $S(s) = diag\,(1, -1)\,[M(s) - I]\,[M(s) + I]^{-1}$. When $b \in [1, \infty)$ and $\lambda \in [0.5, 1)$ (Qin et al., 2020), the relationship $\|S(s)\| \leq 1$ always holds, which means that the teleoperation system based on the modified wave-variable architecture is passive and stable.

With the modified wave-variable architecture, the environmental force F_e is transmitted to the master side in the form of F_m. To achieve the force feedback for the human operator and to reflect the human intention simultaneously, the following master trajectory generator is designed:

$$M_{md}(X_m)\ddot{X}_m + C_{md}(X_m, \dot{X}_m)\dot{X}_m + G_{md}(X_m) = F_h - \nu_m F_m, \tag{S10}$$

where M_{md}, C_{md}, and G_{md} are the desired positive matrixes for the master manipulator, and ν_m is the adjusting factor. Using Eq. (S10), the master position X_m can be generated with the force feedback F_m and the human intention F_h.

Subsequently, the master velocity $\dot{X}_m$ can be obtained by a filter for X_m and then the value of $\dot{X}_m$ is transmitted to the slave side to get the slave reference velocity $\dot{X}_{sr}$ through the modified wave-variable architecture. Thus, by utilizing an integrator, the slave reference position X_{sr} can be obtained.

Considering the different structures of the master and slave manipulators, the following workspace-based asymmetric mapping algorithm is designed, which can be used for the teleoperation of a slave manipulator in both a real underwater environment and a digital simulation platform. For the selected master and slave manipulators, the motion ranges in the X-, Y-, and Z-axes are listed in Table S1. Then, based on Table S1, to ensure that the motion range mapped by the master manipulator can cover that of the slave manipulator as much as possible, the asymmetric mapping algorithm can be defined as follows:

$$X_{sd} = K_1 X_{sr} + K_2, \tag{S11}$$

where $K_1 = diag\{4.7, 4.7, 4.7\}$ and $K_2 = [0.707, -0.322, 0.05]^T$.

Table S1 The motion range of master and slave manipulators

	Master manipulator		Slave manipulator	
	Minimum (m)	Maximum (m)	Minimum (m)	Maximum (m)
X-axis	−0.2115	0.2115	−0.0803	1.3144
Y-axis	−0.1031	0.2847	−1.1185	1.1161
Z-axis	−0.1642	0.0922	−1.1561	1.2300

Furthermore, an RBFNN-based slave controller (Chen et al., 2020) is utilized for the slave manipulator to accurately track the desired trajectory of the slave manipulator X_{sd}:

We define the sliding surface as follows:

$$s_s = \dot{e}_s + \sigma_s e_s, \tag{S12}$$

where $e_s = X_{sd} - X_s$, and $\sigma_s = \sigma_s^T > 0$. Thus, the following equation can be obtained:

$$M_s \dot{s} = -C_s s_s + \vartheta + D_s - T_s - F_e, \tag{S13}$$

where $\vartheta = M_s(\ddot{X}_d + \sigma_s \dot{e}_s) + C_s(\dot{X}_d + \sigma_s e_s) + G_s$.

To ensure the tracking performance of the slave manipulator, T_s is designed as follows:

$$T_s = \kappa_s s_s + \zeta sign(s_s) - F_e + \hat{\vartheta}, \tag{S14}$$

where $\kappa_s > 0$, $\zeta > 0$, and $\hat{\vartheta}$ is the estimated result of ϑ by RBFNN, which can be described as follows:

$$\hat{\vartheta} = \hat{W}_s H_s(z_s) + \epsilon, \tag{S15}$$

where $z_s = \left[\begin{array}{ccccc} e_s^T & \dot{e}_s^T & X_d^T & \dot{X}_d^T & \ddot{X}_d^T \end{array} \right]$, and $\epsilon \leq \bar{\epsilon}$ represents the estimation error.

The updated law of $\hat{W}_s$ is represented as follows:

$$\dot{\hat{W}}_s = \Gamma_s H_s(z_s) s_s^T, \tag{S16}$$

where $\Gamma_s > 0$.

Theorem 1 With the bounded slave desired trajectory X_{rd} and $\zeta \geq \bar{\epsilon} + \bar{d}_s$, by using the controller Eq. (S14) and the updated law in Eq. (S16), the slave subsystem is asymptotically stable with the Lyapunov function as $V_s = \frac{1}{2} s_s^T M_s s_s + \frac{1}{2} tr(\widetilde{W}_s^T \Gamma_s^{-1} \widetilde{W}_s)$, where $\widetilde{W}_s = W_s - \hat{W}_s$.

Remark 1 With the modified wave-variable architecture and the RBFNN-based slave controller in Eq. (S14), the signals transmitted in the whole teleoperation system are bounded, and the overall closed-loop teleoperation is stable under time delays. The transparency of the system can also be improved with the

parameters b and λ in the modified wave-variable architecture, where the slave reference velocity $\dot{X}_{sr}$ can track the master velocity $\dot{X}_m$ with a relatively large b according to Eq. (S7). Subsequently, with the asymmetric mapping algorithm in Eq. (S11) and the controller Eq. (S14), $X_s \to K_1 X_{sr} + K_2$ can be achieved, which means that the slave manipulator is under the guidance of the human operator and can accurately track the desired trajectory. ■

Remark 2 As for the force feedback, through the modified wave-variable architecture, the environmental force F_e in the slave side is transmitted to the master side as F_m. As shown in Eq. (S8), when $\dot{X}_m$ tends to approach zero, the received $F_m(t)$ converges to $F_e(t - T_{sm})$, which means that maintaining slow movement (i.e., with small $\dot{X}_m$) helps reduce the error in force signal. Since it is hard for a human operator to hold the master manipulator at $\dot{X}_m = 0$ permanently, the parameter λ is introduced to suppress the distortion of F_m. Therefore, with a small λ and slow movement on the master side, the parameter F_m can greatly reflect the environmental force F_e. Subsequently, the value of F_m is used in Eq. (S10) to generate the master trajectory X_m, where F_m is served as the force feedback. Thus, by commanding the master manipulator, the human operator can sense the environmental force by using Eq. (S10).

2 Case 2: underwater pipeline docking

Due to the hardware limitation, only one Omni haptic device is selected as the master manipulator 1, while the data of master manipulator 2 is obtained symmetrically to the master manipulator 1. Since a data interface is designed in the digital simulation platform, if there are more than one Omni haptic devices as the master manipulators, the other related teleoperation control algorithms for two collaborating manipulators can be tested and achieved with the data exchange between the digital simulation platform and the actual manipulators.

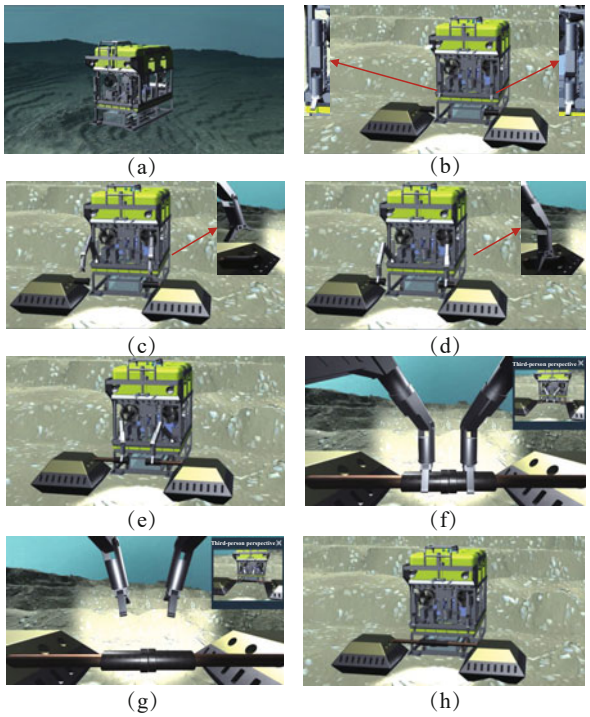

Fig. S2 The underwater pipeline docking process of an ROV in the virtual scene: (a) ROV navigation and motion process; (b) preparing for pipeline grasp; (c) pipeline grasp; (d) preparing for pipeline docking; (e) pipeline docking; (f) completion of pipeline docking; (g) retraction of the two manipulators; (h) return of the two manipulators to the initial positions

The whole underwater pipeline docking process is shown in Fig. S2. Firstly, guided by the ROV navigation-and-motion control unit and the environment perception-and-rebuild unit, the ROV moves from the initial position to the underwater pipeline docking point, as shown in Fig. S2a. Next, as shown in Fig. S2b, when the ROV arrives at the pipeline docking point, its posture is adjusted and the slave manipulator enters the operation mode and is ready to dock. Subsequently, using the teleoperated manipulation unit, the master manipulators are directed to send the position signals of the end effectors to the two slave manipulators via TCP/IP communication mode and command the two slave manipulators to accomplish the tasks, which include the cooperation of the two slave manipulators to grasp the pipeline, perform the pipeline docking, and return to the initial position. During the operation mode, as shown in Figs. S2c and S2d, the docking preparation is first undertaken, whereby the two slave manipulators cooperate to grasp the pipeline on both sides of the underwater base station, and as shown in Figs. S2e-S2h, the two slave manipulators cooperate to dock the pipeline in the docking operation period and return to the initial position when the docking is finished.

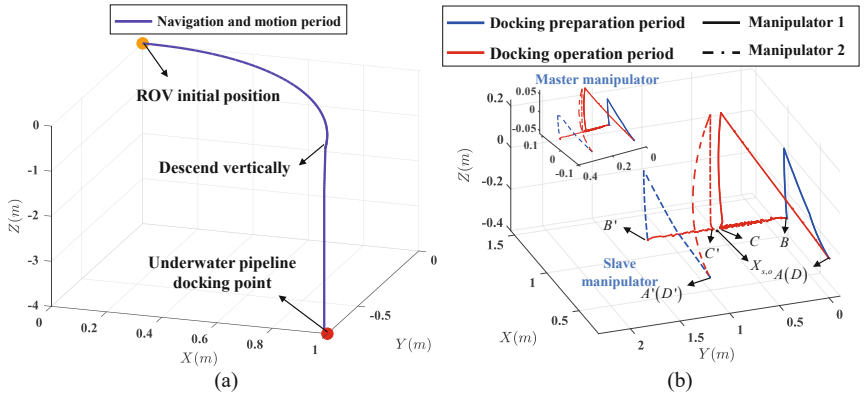

Fig. S3 The motion during operation of the full process of the work-class ROV and its manipulator for the underwater pipeline docking task: (a) the planned practical trajectory of the work-class ROV; (b) the end effector displacement of the teleoperated master and slave manipulators

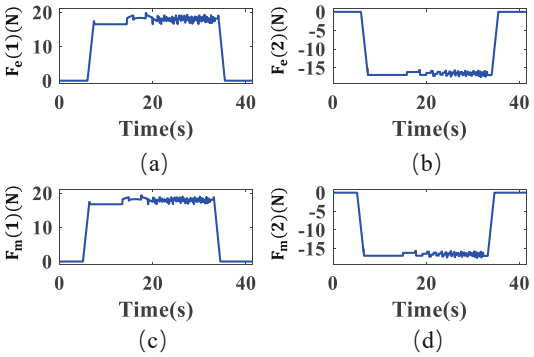

Fig. S4 The environmental force in the underwater pipeline docking process: (a) real environmental force F_e of slave manipulator 1 on the slave side; (b) real environmental force F_e of slave manipulator 2 on the slave side; (c) force feedback F_m of slave manipulator 1 on the master side; (d) force feedback F_m of slave manipulator 2 on the master side

Similarly, the planned practical trajectory of the ROV is shown in Fig. S3a and the end effector displacements of the two master and the two slave manipulators in the underwater pipeline docking operation are shown in Fig. S3b. The relationship among the end effector $X_{s,i}$ of the slave manipulators and the pipeline

docking point $X_{s,o}$ is defined as $X_{s,1} + X_{s,2} = 2X_{s,o}$. In Fig. S3b, the trajectory formed by A(A') and B(B') is the docking preparation period, corresponding to Figs. S2c and S2d. The trajectory formed by B(B'), C(C'), and D(D') is the docking operation period, corresponding to Figs. S2e-S2h.

From Fig.S4, we note that the time delays of the underwater pipeline docking experiment are about 0.5 s; the environmental force feedback for the two slave manipulators are shown in Figs. S4c and S4d, which are also quite the same as the real environmental force shown in Figs. S4a and S4b. In detail, when the manipulators grasp the pipeline (t =5 s), the environmental force increases significantly and is maintained at a certain value during the docking process; when the manipulators start to return to the initial position (t =33 s), the environmental force gradually decreases to zero. Based on the force perception and feedback method, it can be verified that the master manipulator can provide the human operator with the accurate force feedback via the Omni driver.

References

Anderson R, Spong M, 1989. Bilateral control of teleoperators with time delay. *IEEE Trans Automat Contr*, 34(5):494-501. https://doi.org/10.1109/9.24201

Chen Z, Huang FH, Chen WJ, et al., 2020. Rbfnn-based adaptive sliding mode control design for delayed nonlinear multilateral telerobotic system with cooperative manipulation. *IEEE Trans Industr Inform*, 16(2):1236-1247. https://doi.org/10.1109/TII.2019.2927806

Hokayem PF, Spong MW, 2006. Bilateral teleoperation: An historical survey. *Automatica*, 42(12):2035-2057. https://doi.org/10.1016/j.automatica.2006.06.027

Qin L, Huang FH, Chen Z, et al., 2020. Teleoperation control design with virtual force feedback for the cable-driven hyper-redundant continuum manipulator. *Appl Sci*, 10(22). https://doi.org/10.3390/app10228031